

Optical circular dichroism of single-wall carbon nanotubes

Ariadna Sánchez-Castillo

Instituto de Física, Universidad Autónoma de Puebla, Apartado Postal J-48, Puebla 72570, México

C. E. Román-Velázquez and Cecilia Noguez*

Instituto de Física, Universidad Nacional Autónoma de México, Apartado Postal 20-364, D.F. 01000, México

(Received 6 May 2005; revised manuscript received 11 November 2005; published 4 January 2006)

The circular dichroism (CD) spectra of single-wall carbon nanotubes are calculated using a dipole approximation. The calculated CD spectra show features that allow us to distinguish between nanotubes with different angles of chirality, and diameters. These results provide theoretical support for the quantification of chirality and its measurement, using the CD line shapes of chiral nanotubes. It is expected that this information would be useful to motivate further experimental studies.

DOI: [10.1103/PhysRevB.73.045401](https://doi.org/10.1103/PhysRevB.73.045401)

PACS number(s): 78.67.Ch, 81.07.De, 78.20.Bh, 78.40.Ri

I. INTRODUCTION

A century ago Lord Kelvin stated, “I call any geometrical figure, or group of points, chiral, and say that it has chirality, if its image in a plane mirror, ideally realized, cannot be brought to coincide with itself.” According to Kelvin’s definition, one could say only whether an object is chiral or not (achiral), and inferring that chirality is a purely geometrical property, there is no reason to relate it to chemistry, physics, or biology. Decades before, Louis Pasteur had discovered a connection between optical activity and molecular chirality, and found that substances with the same elementary composition have different physical properties; thus, that led him to suppose that forces of nature are not mirror symmetric. Today, we know that chirality plays an important role in chemistry, physics, and biology, and that left amino acids and left peptides are predominant in the living world.^{1,2} Despite the simplicity of Kelvin’s definition, there is not an algorithm for such a criterion to diagnostic chirality.^{3–5} For more than a century, there has been a vast amount of works that have attempted to quantify chirality; however, they have not succeeded yet in finding a universal approach that gives unambiguous results.^{6–14} Furthermore, a drawback of many of these attempts is that they do not provide a way to directly compare the theory to experimental observations.

Among nanostructures, carbon nanotubes are known to be chiral. The atomic structure of single-wall carbon nanotubes (SWNTs) resembles the wrapping of a sheet of carbons located in a two-dimensional hexagonal lattice to form a cylinder. The sheet can be rolled up in different ways, such that nanotubes with similar diameters have different chirality. Despite the fact that the atomic structure of SWNTs is simple, their properties depend dramatically on chirality.¹⁵ SWNTs can be described with a chiral vector \vec{C}_h given by the unit vectors of the hexagonal lattice \vec{a}_1 and \vec{a}_2 , as $\vec{C}_h = n\vec{a}_1 + m\vec{a}_2$, where n and m are integers (see Fig. 1). SWNTs are frequently denoted using these integers as the nanotube (n, m) . The diameter of the nanotube is $d = s/\pi$, where s is the circumferential length of the nanotube, $s = |\vec{C}_h| = a\sqrt{n^2 + m^2 + nm}$, with a the lattice constant of the hexagons. Now, we can define the chiral angle θ_c as the tilt angle of the hexagons

with respect to the direction of the SWNTs axis

$$\cos \theta_c = \frac{\vec{C}_h \cdot \vec{a}_1}{|\vec{C}_h| |\vec{a}_1|} = \frac{2n + m}{2\sqrt{n^2 + m^2 + nm}}. \quad (1)$$

There are only two classes of achiral SWNTs: the armchair with $n=m$ and $\theta_c=30^\circ$, and the zigzag nanotube with $n \neq m$, $m=0$, and $\theta_c=0^\circ$. SWNTs with $0^\circ < \theta_c < 30^\circ$ are all chiral.

It has been shown that linear and circular dichroism (CD) can be useful techniques to study SWNTs.¹⁶ Quantum-mechanical calculations have been performed to study the influence of chirality on the optical properties of SWNTs.^{17–20} Tasaki *et al.*¹⁷ calculated the optical properties of nonrelaxed SWNTs using a tight-binding approach. They found that chiral nanotubes are optically active to circularly polarized light, the CD spectra oscillates and decreases as the diameter of the nanotubes increases. In this work, the authors attribute the origin of the oscillations in the CD spectra to electron transitions among adjacent bands. However, they did not find a relation between the chiral angle and the strength of CD. Recently, Samsonidze *et al.*¹⁸ also employed a tight-binding approach to calculate the electronic transitions for chiral SWNTs and circularly polarized light propagating along the nanotube axis. They found selection rules of

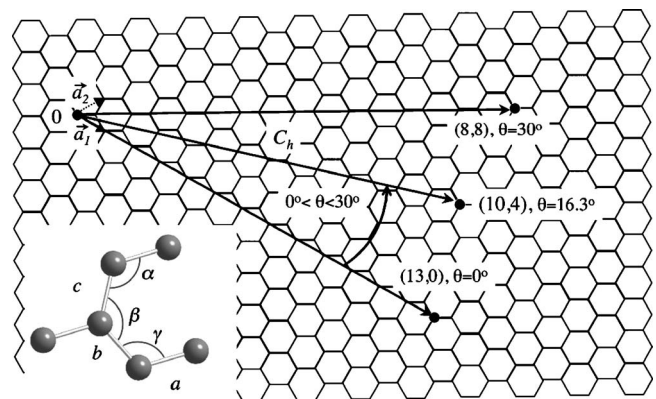


FIG. 1. Model of the atomic geometry of a hexagonal two-dimensional lattice with unit vectors \vec{a}_1 and \vec{a}_2 .

the electronic transitions depending on the handedness of SWNTs, which gives rise to optical activity when the time-reversal symmetry is broken, yielding to CD. They calculated the optical absorption for the nonrelaxed (20,10) SWNT for left- and right-circularly polarized light. From their spectra, it is not possible to infer the behavior of CD, since it is difficult to find differences among them. In both calculations, the tight-binding approximation only accounts for π -band electrons, and other important interactions and effects, such as σ -electrons, many body, and local field, are not included. In fact, it has been found from *ab initio* calculations that σ -electrons, many-body, and local field^{19,20} effects play important roles to determine the optical properties of nanotubes. For example, Marinopoulos *et al.*²⁰ found for small SWNTs of about 4 Å diam, that local field effects dramatically change the response when the electric field is transversal to the symmetry axis. On the other hand, they found that local field effects are insignificant for the parallel polarization. More recently, Chang *et al.*¹⁹ calculated, including excitons, the optical transitions of the (4,2) nanotube for circularly polarized light. They did not find differences between left and right polarizations and concluded that this is a consequence of the system symmetry. However, this result is unlikely because the (4,2) nanotube is chiral and then the system lacks of symmetry.¹⁸ We believe that they did not find differences because they employed a very high-level approach that compromises the numerical accuracy. In fact, quantum-mechanical approaches are still unable to handle these effects for systems with several tens, hundreds, and thousands of atoms due to the huge computational effort that is involved in these sophisticated calculations.

Our goal in this work is to obtain a way to quantify chirality for SWNTs by finding a relation between the chiral angle of SWNTs and their circular dichroism spectra. It is expected that this information would be useful to motivate further experimental studies to correlate distinctive features of the CD spectra with the different angles of chirality and diameters of SWNTs. To explore the capability of the circular dichroism (CD) tool to detect different angles of chirality existing in nanotubes, it would be useful to have a theoretical estimation of their CD behavior. Since the unit cell of SWNTs usually contains hundreds or thousands of atoms, we employ a classical electromagnetic theory, which includes many-body and local field effects in an approximated way to simulate the CD spectra. This classical approximation has been successfully used to study the influence of many-body and local field effects on the optical response at surfaces of covalent semiconductors with cubic symmetry. It was found that the local field at the surface, where the symmetry of the system is broken, is responsible for the observed optical anisotropy.^{21–23} More recently, this classical approach has also been used to study the electron energy-loss spectra of SWNTs.²⁴ Within this classical approximation, the nanotubes are considered as systems composed of coupled-point dipoles, where the polarizability of the dipolar entities are obtained from the dielectric function of bulk graphite. The classical theory employs an *ansatz* in which a localized polarizable unit in the system responds to the external field plus the local field due to all other induced dipole moments at the other sites. This theoretical method can treat systems

of thousands of atoms at a relatively low cost.

II. DIPOLE APPROXIMATION

To study the optical response of nanotubes we employ the point-dipole approximation. This approximation has recently been used to study the optical response of chiral gold nanoclusters,²⁵ as well as the electron energy loss spectra of SWNTs^{24,26} and fullerenes.²⁷

Let us assume that the SWNTs of interest are composed of N carbon atoms represented by a polarizable point dipole located at the position of the atom. We assume that the dipole located at \mathbf{r}_i , with $i=1, 2, \dots, N$, is characterized by a polarizability $\boldsymbol{\alpha}_i(\omega)$, where ω denotes the angular frequency. The SWNT is excited by an incident circular polarized wave with wave vector parallel to the axis of the nanotube. Each dipole is subjected to a total electric field that can be divided into two contributions: (i) $\mathbf{E}_{i,\text{inc}}$, the incident radiation field, plus (ii) $\mathbf{E}_{i,\text{dip}}$, the radiation field resulting from all of the other induced dipoles. The sum of both fields is the so-called local field given by

$$\mathbf{E}_{i,\text{loc}} = \mathbf{E}_{i,\text{inc}} + \mathbf{E}_{i,\text{dip}} = \mathbf{E}_{i,\text{inc}} - \sum_{i \neq j} \mathbf{T}_{ij} \cdot \mathbf{p}_j, \quad (2)$$

where \mathbf{p}_i is the dipole moment of the atom located at \mathbf{r}_i , and \mathbf{T}_{ij} is an off-diagonal matrix, which couples the interaction between dipoles.^{28,29} On the other hand, the induced dipole moment at each atom is given by

$$\mathbf{p}_i = \boldsymbol{\alpha}_i \cdot \mathbf{E}_{i,\text{loc}},$$

such that $3N$ -coupled complex linear equations are obtained from Eq. (2). These equations can be rewritten as

$$\sum_j [(\boldsymbol{\alpha}_j)^{-1} \delta_{ij} + \mathbf{T}_{ij}(1 - \delta_{ij})] \cdot \mathbf{p}_j = \mathbb{M}_{ij} \cdot \mathbf{p}_j = \mathbf{E}_{i,\text{inc}}, \quad (3)$$

where the matrix \mathbb{M} is composed by a diagonal part given by $(\boldsymbol{\alpha}_j)^{-1} \delta_{ij}$ and by an off-diagonal part given by the interaction matrix

$$\mathbf{T}_{ij} \cdot \mathbf{p}_j = \frac{e^{ikr_{ij}}}{r_{ij}^3} \left\{ k^2 \mathbf{r}_{ij} \times (\mathbf{r}_{ij} \times \mathbf{p}_j) + \frac{(1 - ikr_{ij})}{r_{ij}^2} [\mathbf{r}_{ij}^2 \mathbf{p}_j - 3\mathbf{r}_{ij}(\mathbf{r}_{ij} \cdot \mathbf{p}_j)] \right\}. \quad (4)$$

Here, $\mathbf{r}_{ij} = \mathbf{r}_i - \mathbf{r}_j$, $r_{ij} = |\mathbf{r}_{ij}|$ and k is the magnitude of the wave vector of the incident electromagnetic field.

The diagonal part in Eq. (3) is related to the polarizability of each dipolar entity (i.e., to the material properties of the system), while the off-diagonal part depends only on the atomic positions (i.e., on the geometrical properties). Once we solve the complex-linear equations shown in Eq. (3), the dipole moment on each atom in the nanotube can be determined, and then we can calculate the extinction cross section C_{ext} of the SWNT. In terms of the dipole moments,^{28,29}

$$C_{\text{ext}} = \frac{4\pi k}{E_0^2} \sum_{i=1}^N \text{Im}(\mathbf{E}_{i,\text{inc}}^* \cdot \mathbf{p}_i), \quad (5)$$

where (*) means complex conjugate.

Circular dichroism is defined as the differential absorption of left (L) and right (R) hand circularly polarized light, which is obtained by subtracting the corresponding extinction efficiencies, Q_{ext} , as

$$CD = Q_{\text{ext}}^{\text{R}} - Q_{\text{ext}}^{\text{L}}. \quad (6)$$

Here, the extinction efficiency is defined as $Q_{\text{ext}} = C_{\text{ext}}/A$, where $A = \pi sL$ and L is the length of the unit cell of the nanotube. Edge effects due to the finite length of the nanotube are removed by using periodic boundary conditions. If the handedness of the nanotube is changed according to definition of Ref. 18, we have, $Q_{\text{ext}}^{\text{R}} \rightarrow Q_{\text{ext}}^{\text{L}}$, and $Q_{\text{ext}}^{\text{L}} \rightarrow Q_{\text{ext}}^{\text{R}}$, such that CD will change just in sign. This is also observed in Fig. 3 of Ref. 18.

Because chirality is a geometrical property, the CD spectrum will be more sensitive to the second term inside the bracket in Eq. (3), which depends on the atomic geometry, than to the first one related to the polarizability. Therefore, the simulated CD spectra will include the geometrical information about the chiral SWNTs. We find that is crucial for the simulated CD spectra to have “realistic” atomic positions to obtain the right curvature and helicity of each SWNTs studied here. We will see in Sec. IV that the differences among the extinction efficiencies for left- and right-circularly polarized light are of the order of 10^{-6} . If nonrelaxed atomic positions are used to calculate CD, the intensity of the spectra is very small, such that the accuracy of our numerical calculations becomes compromised. On the other hand, when relaxed atomic positions are considered, the curvature and helicity are improved up to 5% with respect to the nonrelaxed positions, the CD spectra are more intense, and numerical errors become negligible. Note that if we only calculate the extinction or absorption efficiencies, we do not find visible differences among the spectra obtained using nonrelaxed or relaxed atomic positions. In conclusion, it will be important to obtain relaxed atomic positions of SWNTs only if we want to do a systematic study of their CD.

In this work, we assume that the polarizability for each entity α_i is isotropic and is the same for all the point dipoles in the nanotube ($\alpha_i = \alpha_j \equiv \alpha$). We obtain this polarizability from the Clausius-Mossotti relation, from which the dielectric function of the system was taken from the experimental data for graphite.³⁰ We shall point out that the dielectric function of graphite does not contain the information due to quantum confinement and excitonic effects observed in SWNTs.³²⁻³⁴ However, the dipole model is still appropriated if one is interested in knowing the general behavior of CD. Of course, if one is able to include those effects, maybe using experimental measurements or realistic calculations of the dielectric functions, quantum confinement, and excitonics will play an important role, even more if the selection rules of the electron transitions are determined by chirality. Note that this polarizability cannot be associated with the corresponding atomic polarizability because, to find a relationship between them, it is necessary to consider the confinement of each atom by the rest of the atoms, multipolar, van der Waals, and other interactions.²¹ However, this approximation has been successfully employed to study the influence of the breaking of the symmetry on the optical

properties at surfaces of cubic covalent semiconductors.²¹⁻²³ For these cubic covalent crystals, it has been found that the best location of the polarizable entities are along the bonds, and the polarizabilities are anisotropic.^{22,23} In our case, we find that the simplest and best representation corresponds to the dipolar entities located at the atomic positions.³¹ This representation has been used before to study optical properties of carbon nanotubes and fullerenes, providing good qualitative agreement with experimental data.^{24,26,27} We believe that the symmetry of the crystal is important to choose the location of the point dipoles.

III. ATOMIC STRUCTURES

We obtained the atomic structures of the SWNTs within the density-functional theory (DFT) using the SIESTA computer code.³⁵ This code has been widely employed to study the atomic relaxation and electronic properties of small SWNTs.³⁶⁻³⁹ We used Perdew-Burke-Ernzerhof exchange-correlation functional⁴⁰ within the generalized gradient approximation (GGA). To take into account the interaction between valence electrons and ionic cores, we employed fully nonlocal norm-conserving pseudopotentials proposed by Troullier and Martins.⁴¹ A double ζ polarized (DZP) basis set was used with cutoff radii of 5.12 and 6.25 atomic units for the $2s$ and $2p$ orbitals, respectively. In this work, we consider that SWNTs are infinitely long by repeating the unit cell of length L along the nanotube axis. More details of the theoretical model employed here can be found elsewhere.³⁶⁻³⁹

In Table I, we summarized the geometrical parameters obtained in this work using SIESTA, as labeled in Fig. 1. For comparison, we also include the corresponding parameters of the nonrelaxed SWNTs. The geometries were relaxed until remanent forces were <0.01 eV/Å. After relaxation, we found that the chiral vector and diameter of the nanotubes increase by $<2\%$ with respect to their corresponding nonrelaxed (n.r.) values. The bond length in the radial direction, denoted by a in Fig. 1, changes more than the bond lengths in the directions parallel to the axis of SWNTs. These bonds are denoted by b and c in Fig. 1. For SWNTs with diameters of ~ 1 nm, the bond lengths a and c are similar and always larger than b . For SWNTs with larger diameters, the bond lengths a , b , and c become almost equal. The unit cell length L is also deviated from its nonrelaxed value, increasing $\sim 1\%$ in all cases. Then, the bond angles (see Fig. 1) are also modified upon relaxation, such that the α angle is larger, while the β and γ angles tend to be reduced. Our results of the atomic geometry of SWNTs are in excellent agreement with previous DFT calculations for SWNTs with small diameters,³⁶⁻³⁹ and with tight-binding results for large nanotubes.^{42,43} We also performed DFT calculations within the local density approximation using the same approximations as in Ref. 36, and the only difference with the atomic parameters is a constant difference in the bond length, which is about 1% smaller. This difference does not change the results of the CD spectra, as we will discuss later.

IV. CIRCULAR DICHROISM SPECTRA

We present results for the extinction efficiency and circular dichroism spectrum of different SWNTs. The spectra

TABLE I. Geometrical parameters as defined in Fig. 1 for relaxed and nonrelaxed (n.r.) SWNTs. θ_c , α , β , and γ are given in degrees.

(n,m) (n.r.)	θ_c	$ C_h $ (Å)	a (Å)	b (Å)	c (Å)	α	β	γ
(13,1)	3.6	34.46	1.46	1.45	1.46	118.8	120.0	119.9
		33.74	1.44	1.44	1.44	118.6	120.1	120.0
(26,2)	3.6	10.87	1.45	1.45	1.46	119.7	120.0	120.0
		10.74	1.44	1.44	1.44	119.6	120.0	120.0
(11,2)	8.5	30.76	1.46	1.45	1.46	118.5	120.0	119.8
		30.24	1.44	1.44	1.44	118.3	119.9	120.1
(12,3)	10.9	34.80	1.46	1.46	1.46	118.9	119.9	119.8
		34.29	1.44	1.44	1.44	118.7	120.1	119.9
(20,5)	10.9	57.84	1.46	1.45	1.46	119.6	120.0	119.9
		57.11	1.44	1.44	1.44	119.5	120.0	119.5
(36,9)	10.9	103.95	1.45	1.45	1.46	119.9	120.0	120.0
		102.87	1.44	1.44	1.44	119.8	120.0	120.0
(10,4)	16.1	31.67	1.46	1.45	1.46	118.8	119.8	119.7
		31.15	1.44	1.43	1.44	118.6	120.1	119.7
(20,8)	16.1	63.05	1.46	1.45	1.46	119.7	120.0	119.9
		62.30	1.44	1.44	1.44	119.7	120.0	119.9
(30,12)	16.1	94.71	1.47	1.47	1.47	119.9	120.0	120.0
		93.45	1.44	1.44	1.44	119.8	120.0	120.0
(10,5)	19.1	33.52	1.46	1.45	1.46	119.0	119.8	119.7
		32.99	1.44	1.43	1.44	118.9	120.1	119.7
(20,10)	19.1	66.76	1.46	1.46	1.46	119.8	120.0	119.9
		65.97	1.44	1.44	1.44	119.7	120.0	119.9
(30,15)	19.1	100.03	1.45	1.45	1.46	119.9	120.0	120.0
		98.96	1.44	1.44	1.44	119.9	120.0	120.0
(8,5)	22.4	28.84	1.46	1.45	1.46	118.9	119.6	119.5
		28.33	1.44	1.43	1.44	118.6	119.4	120.0
(8,6)	25.3	30.85	1.46	1.45	1.46	119.1	119.6	119.6
		30.34	1.44	1.43	1.44	118.9	119.4	120.0

were calculated using the dipole approximation introduced in Sec. II, and the atomic positions of SWNTs as obtained in Sec. III. We first present results for the extinction efficiency of SWNTs as a function of the frequency. Then, we discuss the CD spectra for different SWNTs with the same diameter but different chirality, and finally, the CD spectra for SWNTs with the same chirality but different diameter.

In Fig. 2, we show the extinction efficiency Q_{ext} in arbitrary units for the SWNT (13,1), as a function of the photon energy of the incident light from 2 eV (620 nm) to 8 eV (155 nm). We observe that Q_{ext} has a maximum at 6.2 eV, where absorption effects are dominant, while the asymmetry of the peak is due to scattering effects because the SWNTs considered here are infinitely long. Therefore, a chiral SWNT will show dichroism around these energies. We only show the Q_{ext} for one SWNT; however, the same behavior is observed for the rest of the nanotubes studied here.

Samsonidze *et al.*¹⁸ recently calculated the absorption spectrum of the (20,10) nanotube within a tight-binding approach and using a small basis of atomic orbitals, where only

p_z electrons were considered. They found a sharp peak at around 2.6 eV. However, since they used such a small basis set, it is expected that conduction bands are not well described and electron transitions could be at different energies that they must be. We also note that the peak is very sharp because they did not consider interactions between different

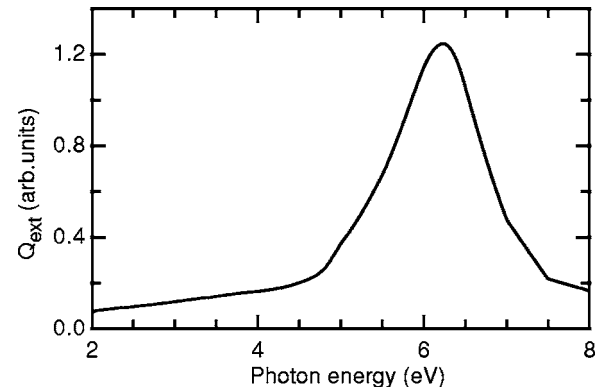


FIG. 2. Extinction efficiency of the SWNT (13,1).

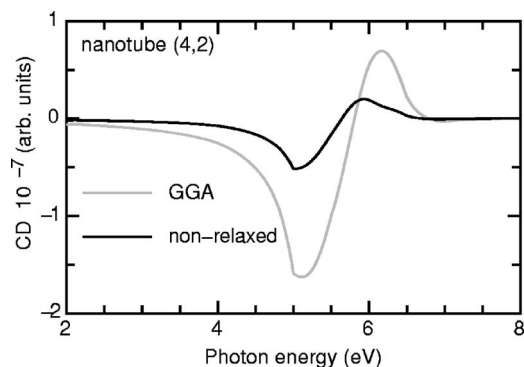


FIG. 3. CD spectra of (4,2) nanotube using nonrelaxed and relaxed atomic positions.

kind of orbitals, and many-body and local field effects are completely ignored. Chang *et al.*¹⁹ calculated the optical transitions including excitonic effects of the (4,2) nanotube for circularly-polarized light. As mentioned before, they did not find differences between the absorption from left and right polarizations, and concluded that this is because of the symmetry of the system. But this result is unlikely because the (4,2) nanotube is chiral and then the system lacks of symmetry.¹⁸ We believe that they did not find differences because they employed a very high-level approach such that its numerical accuracy might be of the same order of the differences. In such a case, errors due to numerical rounding could hide the chirality effects. In conclusion, a comparison of our calculations to previous results cannot be done in a direct way.

We calculate the CD spectra for all the nanotubes listed in Table I. We found that the differences of the extinction efficiencies between left- and right-polarized light are of the order of 10^{-6} . Since these differences are quite small, we found that the spectra are sensitive to the details on the atomic positions. For example, if we use the nonrelaxed structures, the CD spectra are less intense and we do not find any relation with the chiral angle. We also test some nanotubes that were relaxed using DFT within the local-density approximation. In this case, we obtain essentially the same curvature and helicity for the nanotubes but with bond lengths slightly smaller (differences of $\sim 1\%$). In this case, CD spectra do not differ from GGA results, and we find the same tendency as we will discuss below. For achiral nanotubes, armchair ($\theta_c=30^\circ$) and zigzag ($\theta_c=0^\circ$), the CD spectra is always null, being the differences between left- and right-polarized light four orders of magnitude smaller than for chiral SWNTs. In Fig. 3, we compare the CD spectra of the (4,2) nanotube for nonrelaxed and relaxed atomic coordinates within DFT-GGA. The intensity of CD is one order of magnitude smaller for the nonrelaxed structure.

In Fig. 4, we present the CD spectra for SWNTs of about the same diameter, $d=1$ nm, but different chiral angle θ_c . We show the CD in arbitrary units as a function of the photon energy of the incident light from 2 to 8 eV. All the spectra show a minimum at 5.2 eV (238 nm), and a maximum at 6.1 eV (203 nm), where light absorption of graphite is more intense.³⁰ From Fig. 4(a), we observe that the CD spectrum is more intense as the chiral angle increases, while in Fig.

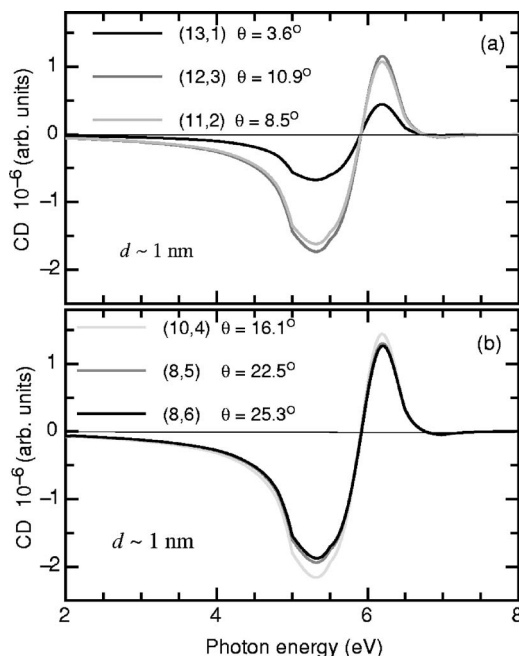


FIG. 4. CD spectra of SWNTs with the same diameter $d = 1$ nm and (a) $0^\circ \leq \theta_c \leq 15^\circ$, and (b) $15^\circ \leq \theta_c \leq 30^\circ$.

4(b) the contrary is observed. We found that the maximum intensity of the CD spectra is reached when the helicity of the nanotubes is also a maximum, i.e., when θ_c is close to 15° , as shown in the nanotube structures in Fig. 5. For all diameters of SWNTs, we find the same behavior of the CD spectrum as a function of the chiral angle. In summary, we obtain that the intensity of the CD spectrum is directly related to the chiral angle of the SWNT. Therefore, we can conclude that CD measurements can be useful to quantify chirality in these nanostructures.

Now, we analyze the CD spectra for nanotubes of different diameter but the same chiral angle. In Fig. 6, we show the CD spectra for nanotubes with (a) $\theta_c=10.9^\circ$ and diameters $d=1.1, 1.8,$ and 3.3 nm; with (b) $\theta_c=16.1^\circ$ and diameters $d=1.0, 2.0,$ and 3.0 nm, and with (c) $\theta_c=19.1^\circ$ and diameters $d=1.1, 2.1,$ and 3.1 nm. For the three cases, we

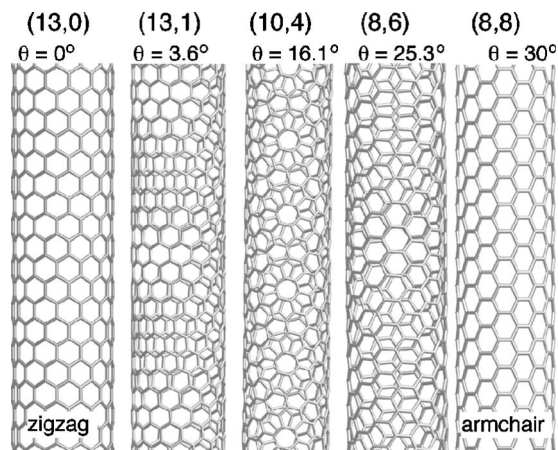


FIG. 5. Structure of single-wall SWNTs with different chiral angles between 0° and 30° .

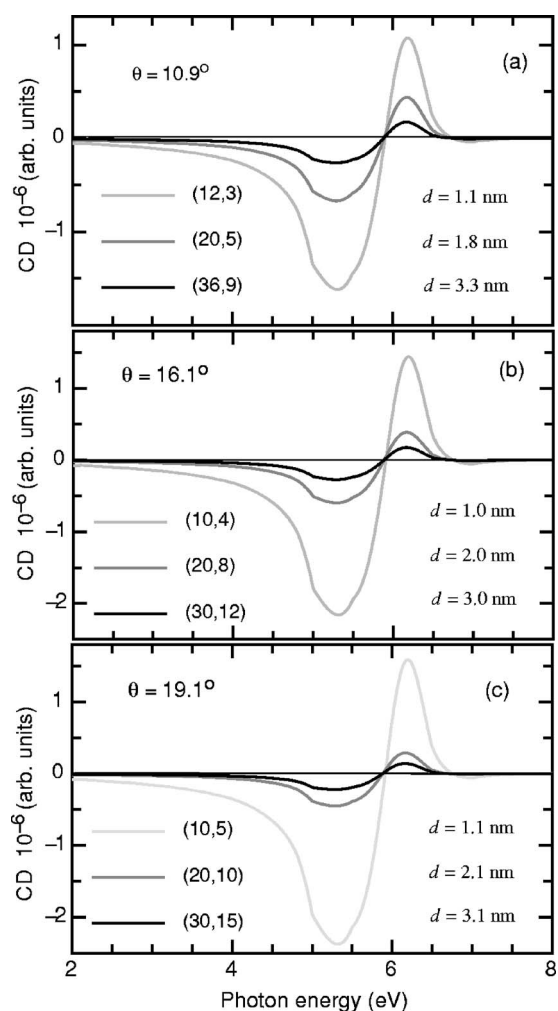


FIG. 6. CD spectra of SWNTs of different diameter but same chiral angle (a) $\theta_c = 10.9^\circ$, (b) $\theta_c = 16.1^\circ$, and (c) $\theta_c = 19.1^\circ$.

found that the intensity of the CD spectrum is always larger for smaller diameters. We observe that the maximum of the CD spectra is about half (one-third) when the diameters is twice (three times) larger. This is due to the fact that wider nanotubes with the same helicity have a larger surface, such that the chiral effect is less intense. In the limit case, when the diameter goes to infinity and we recover the hexagonal sheet, the CD will be zero even when θ_c will remain unchanged. These observations were also reported by Tasaki *et*

al.,¹⁷ where they found that the intensity of the CD spectra diminishes as the diameter of the nanotubes increases. In summary, we found that there is a relation between the intensity of the CD spectra with the diameter of the nanotube. From these results, we can conclude that CD measurements can be also useful to quantify the diameter of chiral SWNTs. Unfortunately, we have not found a way to disentangle the CD variations due to the changes of both chiral angle and diameter. However, the present results can be useful when the nanotubes are fabricated with a well-defined diameter, as, for example, those grown using templates and porous matrices.⁴⁴ Taking into account that in such templates SWNTs are not completely aligned, it would be possible to observe the effect, since the intensity is affected in about 30%, when the axes of nanotubes are off-aligned in average 30° .

V. CONCLUSIONS

Using the computer code called SIESTA, within the density-functional theory, we obtained the atomic positions of 14 different single-wall carbon nanotubes, chosen such that most of them were not reported before in the literature. Our DFT results are in excellent agreement with previous calculations of smaller single-wall carbon nanotubes. Furthermore, we have studied the circular dichroism optical spectra of these single-wall carbon nanotubes of different diameters and chirality within a dipole approximation. We found that, for nanotubes with a given diameter, the intensity of circular dichroism spectra increases as the helicity of the nanotube also does. We also found that the intensity of the circular dichroism spectra of single-wall nanotubes, for a given chiral angle, depends on the diameter of the nanotube, such that wider nanotubes show a less intense spectra. From these results, we can conclude that circular dichroism measurements can be useful to quantify chirality as well the diameters of chiral SWNTs. It is expected that this information would be useful to motivate further experimental studies in this direction.

ACKNOWLEDGMENTS

We acknowledge the fruitful discussion with Ignacio L. Garzón and Lilia Meza Montes. Partial financial support from DGAPA-UNAM Grant No. IN101605, and VIEP-BUAP II 193-04/EXC/G is also acknowledged.

*Corresponding author. Email: cecilia@fisica.unam.mx

¹L. D. Barron, *Nature (London)* **405**, 895 (2000).

²G. L. J. A. Rikken and E. Raupach, *Nature (London)* **405**, 932 (2000).

³B. B. Smirnov, O. V. Lebedev, and A. V. Evtushenko, *Acta Crystallogr., Sect. A: Found. Crystallogr.* **A55**, 790 (1999).

⁴A. B. Buda and K. Mislow, *J. Am. Chem. Soc.* **114**, 6006 (1992).

⁵L. Bellarosa and F. Zerbetto, *J. Am. Chem. Soc.* **125**, 1975 (2003).

⁶W. J. Richter, B. Richter, and E. Ruch, *Angew. Chem.* **85**, 20 (1973).

⁷T. Damhus and C. E. Schäffer, *Inorg. Chem.* **22**, 2406 (1983).

⁸L. A. Kutulya, V. E. Kuz'min, I. B. Stel'makh, T. V. Handri-mailova, and P. P. Shtifanyuk, *J. Phys. Org. Chem.* **5**, 308 (1992).

⁹H. Zabrodsky, S. Peleg, and D. Avnir, *J. Am. Chem. Soc.* **114**, 7843 (1992); **115**, 8278 (1993); **117**, 462 (1995).

¹⁰G. Moreau, *J. Chem. Inf. Comput. Sci.* **37**, 929 (1997).

- ¹¹J. Maruani, G. Gilat, and R. Veysere, C. R. Acad. Sci., Ser. IIB Mec. **319**, 1165 (1994).
- ¹²P. E. auf der Heide Thomas, A. B. Buda, and K. Mislow, J. Math. Chem. **6**, 255 (1990).
- ¹³M. Nogradi, *Stereoselective Synthesis: A Practical Approach*, (Wiley-VCH, Weinheim, 1995).
- ¹⁴V. I. Sokolov and N. F. Standen (translator), *Introduction to Theoretical Stereochemistry* (Gordon & Breach, New York, 1991).
- ¹⁵R. Saito, G. Dresselhaus, and M. S. Dresselhaus, *Physical Properties of Carbon Nanotubes* (Imperial College Press, London, 1998).
- ¹⁶J. Rajendra, M. Baxendale, L. G. Dit Rap, and A. Rodger, J. Am. Chem. Soc. **126**, 11182 (2004).
- ¹⁷S. Tasaki, K. Maekawa, and T. Yamabe, Phys. Rev. B **57**, 9301 (1998).
- ¹⁸G. G. Samsonidze, A. Grüneis, R. Saito, A. Jorio, A. G. Souza Filho, G. Dresselhaus, and M. S. Dresselhaus, Phys. Rev. B **69**, 205402 (2004).
- ¹⁹E. Chang, G. Bussi, A. Ruini, and E. Molinari, Phys. Rev. Lett. **92**, 196401 (2004).
- ²⁰A. G. Marinopoulos, L. Reining, A. Rubio, and N. Vast, Phys. Rev. Lett. **91**, 046402 (2003).
- ²¹W. L. Mochán and R. G. Barrera, Phys. Rev. Lett. **55**, 1192 (1985).
- ²²B. S. Mendoza and W. L. Mochán, Phys. Rev. B **53**, R10473 (1996).
- ²³C. D. Hogan and C. H. Patterson, Phys. Rev. B **57**, 14843 (1998).
- ²⁴A. Rivacoba and F. J. García de Abajo, Phys. Rev. B **67**, 085414 (2003).
- ²⁵C. E. Román-Velázquez, C. Noguez, and I. L. Garzón, J. Phys. Chem. B **107**, 12035 (2003).
- ²⁶X. H. Wu, L. S. Pan, H. Li, X. J. Fan, T. Y. Ng, D. Xu, and C. X. Zhang, Phys. Rev. B **68**, 193401 (2003).
- ²⁷L. Henrard and Ph. Lambin, J. Phys. B **29**, 5127 (1996).
- ²⁸E. M. Purcell and C. R. Pennypacker, Astrophys. J. **186**, 705 (1973).
- ²⁹B. T. Draine, Astrophys. J. **333**, 848 (1998).
- ³⁰D. L. Greenaway, G. Harbeke, F. Bassani, and E. Tosatti, Phys. Rev. **178**, 1340 (1969).
- ³¹We also did calculations when the dipolar moments are located along the bonds and are anisotropic, i.e., using prolate spheroids instead of spheres. In this case, we found the same results as when the dipoles are at the atoms. However, for the spheroidal system it is necessary to introduce a parameter in order to find the anisotropy factor. Therefore, we choose the spheres located at the atoms in order to handle a simpler system.
- ³²C. D. Spataru, S. Ismail-Beigi, L. X. Benedict, and S. G. Louie, Phys. Rev. Lett. **92**, 077402 (2004).
- ³³R. B. Weisman and S. M. Bachilo, Nano Lett. **3**, 1235 (2003).
- ³⁴C. Fantini, A. Jorio, M. Souza, M. S. Strano, M. S. Dresselhaus, and M. A. Pimenta, Phys. Rev. Lett. **93**, 147406 (2004).
- ³⁵S. Sánchez-Portal, P. Ordejón, E. Artacho, and J. M. Soler, Int. J. Quantum Chem. **65**, 453 (1997).
- ³⁶M. Machón, S. Reich, C. Thomsen, D. Sánchez-Portal, and P. Ordejón, Phys. Rev. B **66**, 155410 (2002).
- ³⁷S. Reich, C. Thomsen, and P. Ordejón, Phys. Rev. B **65**, 153407 (2002).
- ³⁸S. Reich, C. Thomsen, and P. Ordejón, Phys. Rev. B **65**, 155411 (2002).
- ³⁹S. Reich, C. Thomsen, and P. Ordejón, Phys. Rev. B **64**, 195416 (2001).
- ⁴⁰J. P. Perdew, K. Burke, and M. Ernzerhof, Phys. Rev. Lett. **77**, 3685 (1996).
- ⁴¹N. Troullier and J. L. Martins, Phys. Rev. B **43**, 1993 (1991).
- ⁴²V. N. Popov, New J. Phys. **6**, 17 (2004).
- ⁴³G. G. Samsonidze, R. Saito, N. Kobayashi, A. Grüneis, J. Jiang, A. Jorio, S. G. Chou, G. Dresselhaus, and M. S. Dresselhaus, Appl. Phys. Lett. **85**, 5703 (2004).
- ⁴⁴Z. M. Li, Z. K. Tang, H. J. Liu, N. Wang, C. T. Chan, R. Saito, S. Okada, G. D. Li, J. S. Chen, N. Nagasawa, and S. Tsuda, Phys. Rev. Lett. **87**, 127401 (2001).